Members of a highly widespread bacteriophage family are hallmarks of metabolic syndrome gut microbiomes

Patrick A. de Jonge[1†], Koen Wortelboer[1†], Torsten P.M. Scheithauer[1], Bert-Jan H. van den Born[1], Aeilko H. Zwinderman[2], Franklin L. Nobrega[3], Bas E. Dutilh[4], Max Nieuwdorp[1], Hilde Herrema[1*]

[1]: Departments of Internal and Experimental Vascular Medicine, Amsterdam University Medical Centers, Location AMC, Amsterdam, The Netherlands

[2]: Department of Clinical Epidemiology, Biostatistics and Bioinformatics, Amsterdam University Medical Centers, Location AMC, University of Amsterdam, Amsterdam, The Netherlands

[3]: School of Biological Sciences, Faculty of Environmental and Life Sciences, University of Southampton, Southampton, United Kingdom

[4]: Theoretical Biology and Bioinformatics, Science for Life, Utrecht University, Utrecht, the Netherlands

[†]: These authors contributed equally to this work.

[*]Correspondence: h.j.herrema@amsterdamumc.nl

Keywords: Metabolic Syndrome, Gut microbiome, Gut virome, Bacteriophage, Metagenomics

Summary

There is significant interest in altering the course of cardiometabolic disease development via the gut microbiome. Nevertheless, the highly abundant viral members -which impact gut bacteria- of the complex gut ecosystem remain understudied. Here, we characterized gut virome changes associated with metabolic syndrome (MetS), a highly prevalent clinical condition preceding cardiometabolic disease. MetS gut virome populations exhibited decreased richness and diversity, but larger inter-individual variation. These populations were enriched in phages infecting *Bacteroidaceae* and depleted in those infecting *Ruminococcaeae*. Differential abundance analysis

identified eighteen viral clusters (VCs) as significantly associated with either MetS or healthy viromes. Among these are a MetS-associated *Roseburia* VC that is related to healthy control-associated *Faecalibacterium* and *Oscillibacter* VCs. Further analysis of these VCs revealed the *Candidatus Heliusviridae*, a highly widespread gut phage lineage found in 90+% of the participants. The temperate *Ca. Heliusviridae* are important novel research targets for understanding the role of the microbiome in human cardiometabolic health and developing microbiome-targeted interventions.

Introduction

The human gut microbiome influences many (metabolic) processes, including digestion, the immune system[1], and endocrine functions[2]. It is also involved in diseases such as type 2 diabetes[3], fatty liver disease[4] and inflammatory bowel disease[5]. Though studies of these gut microbiome effects on health and disease mostly focus on bacteria, increasing attention is devoted to bacteriophages (or phages).

Phages are viruses that infect bacteria. By infecting bacteria, they can significantly alter gut bacterial communities, mainly by integrating into bacterial genomes as prophages (lysogeny) or killing bacteria (lysis). Such alterations to bacterial communities in turn affect the interactions between bacteria and host, making phages part of an interactive network with bacteria and hosts. For example, an increase in phage lytic action is linked to decreased bacterial diversity in inflammatory bowel disease[6,7], prophage integration into *Bacteroides vulgatus* modifies bacterial bile acid metabolism[8], and dietary fructose intake prompts prophages to lyse their bacterial hosts[9].

Gut virome alterations have been linked to several disease states like inflammatory bowel diseases[6,7], malnutrition[10], and type 2 diabetes[11]. But many such studies have not been able to identify specific viral lineages that are involved in such diseases, mainly due to the lack of viral marker genes[12,13] and high phage diversity due to the rapid evolution[14]. Consequently, human gut phage studies are limited to relatively low taxonomic levels. While recent efforts uncovered viral families that are widespread in human populations, such as the crAss-like[15,16] phages, these have not been successfully linked to disease states. In order to develop microbiome-targeted interventions to benefit human health, it is pivotal to study such higher-level phage taxonomies in the gut among relevant cohorts.

Here, we report on gut virome alterations in metabolic syndrome (MetS)[17] among 196 people. MetS is a collection of clinical manifestations that affects about a quarter of the world population, and is a major global health concern because it can progress into cardiometabolic diseases like type 2 diabetes, cardiovascular disease, and non-alcoholic fatty liver disease[18,19]. As the gut microbiome is increasingly seen as a contributing agent of MetS[20–22], it has great potential to study gut virome alterations in relation to health. We found MetS-connected decreases in virome richness and diversity, which are correlated to bacterial population patterns. Such correlations extended to the abundance of phages and their particular bacterial hosts. We further identified eighteen phages that are significantly correlated with either MetS or healthy controls. We found that three of these phages, one correlated with MetS and two with controls, are related. These are members of the *Candidatus Heliusviridae*, a previously unstudied lineage of temperate *Clostridiales* phages that is present in over 90% of the participants. Phylogenetic and taxonomic classification revealed at least six distinct *Ca. Heliusviridae* sub-groups, two of which are significantly more abundant in MetS. As the *Ca. Heliusviridae* include both phages which are associated with MetS and with healthy controls, this extremely widespread lineage is an interesting target for research into the human gut virome and development of therapeutic agents that alter microbiome communities.

Results

Metagenomic sequencing identifies high divergence in MetS viromes

We performed bulk metagenome sequencing on fecal samples of 97 MetS and 99 healthy participants from the Healthy Life in an Urban Setting (HELIUS) cohort[23], a large population study in Amsterdam, the Netherlands (**Supplementary Table 1**). This yielded an average of 42.1 ± 6.7 million reads per sample (median: 40.6 million reads). We assembled reads and selected 6,780,412 contigs longer than 1,500 bp or shorter but circular, among which we predicted viral sequences that we clustered at 95% nucleotide identity. This produced a database of 25,894 non-redundant viral contigs, which we grouped by shared protein content[24] into 2,866 viral clusters (VCs). These comprised 14,434 contigs, while the remainder were singletons too distinct to

confidently cluster with other viral contigs. Treating such singletons as VCs with one member gave a final dataset of 14,326 VCs.

Analysis of the read depth per VC across participants (**Supplementary Table 2**) underscored the extremely high inter-individual diversity in gut viromes, as 8,799 VCs (61.4% of total VCs) were specific to a single individual and 5,122 VCs (35.8% of total VCs) were found in two to twenty participants (*i.e.*, fewer than 10% of participants, **Supplementary Figure 1a**). Due to being so common, these two sets of VCs also comprised a mean of 92.6 ± 4.4% (median: 93.5%) of total viral abundance (**Supplementary Figure 1b**). The remaining 241 VCs (1.7%) were present in over 10% of participants and represented 7.4 ± 4.4% (median: 6.6%) of total viral abundance. Of these, 27 (0.2%) were found in over 30% of participants and may be part of the core human gut virome[25].

Next, we examined the abundance the of four VC sets (*i.e.*, individual-specific, present in ≤10, 10-30% and ≥30% of participants) in individual participants. Intriguingly, for all four sets both the participant with the highest and lowest relative abundance had MetS (**Supplementary Figure 1c**). This suggested greater variation among MetS viromes than those in healthy controls, which we confirmed with a permutational analysis of multivariate dispersions (permdisp) on Bray-Curtis dissimilarities ($p = 0.003$, **Supplementary Figure 1d**). In conclusion, while we found high inter-individual diversity among viromes in all participants, MetS viromes exhibited greater variety.

<u>Viral and bacterial gut populations are depleted in MetS</u>

To gain a deeper understanding of MetS virome community dynamics, we first examined total viral abundance. Total read fractions that mapped to VCs were lower in MetS than controls, indicating wholesale depletion of MetS viromes (Wilcoxon signed rank test, $p = 0.013$, **Supplementary Figure 2a**). This pattern extended to prophage-carrying bacterial contigs, which likewise were less abundant among MetS participant than controls (Wilcoxon signed rank test, $p = 1.4 \times 10^{-4}$, **Supplementary Figure 2b**). This notably did not reflect a depletion in temperate phages, as the abundance of VCs that encode the integrases used in prophage formation were unaltered (Wilcoxon signed rank test, $p = 0.47$, **Supplementary Figure 2c**). We hypothesize that prophage formation rates among MetS viromes decrease and that phages possibly more commonly utilize the lytic phage life cycle.

For further analysis of viral communities, we examined virome richness and diversity. We determined viral richness by measuring the number of VCs that were present (*i.e.*, had a relative abundance above 0) in each participant, using a horizontal coverage cutoff of 75%[26]. This showed that besides lower total viral abundance, MetS viromes also had lower viral richness than controls, but equal evenness (Wilcoxon signed rank test, richness $p = 8.7 \times 10^{-8}$, Pielou evenness $p = 0.79$, **Figure 1a** and **b**). Nevertheless, due to the strong differences in species richness, viral α-diversity was significantly decreased among MetS participants (Shannon H' $p = 1.3 \times 10^{-3}$, **Figure 1c**). This suggested that MetS gut viromes are distinct from healthy communities. Indeed, MetS and control viromes displayed significant separation when assessed by principal covariate analyses (PCoA) of β-diversity based on Bray-Curtis dissimilarities (permanova $p = 0.001$, **Figure 2d**).

Because phages are obligate parasites of bacteria, we also studied bacterial 16s rRNA amplicon sequencing data. This showed that MetS viromes mirror bacterial communities in species richness and α-diversity, but not evenness, which was significantly lowered in MetS bacterial populations (Wilcoxon signed rank test, Chao1 richness $p = 9.1 \times 10^{-4}$, Shannon H' $p = 1.5 \times 10^{-15}$, Pielou evenness $p = 1.8 \times 10^{-14}$, **Supplementary Figure 3a-c**). Additionally, bacterial communities separated in PCoA analysis in similar fashion to viromes (permanova $p = 0.001$ for both bacteria and phages, **Supplementary Figure 3d**). Population-level virome changes in MetS are thus directly related to a depletion of host bacteria populations, an assertion strengthened by significant direct correlations between viral and bacterial communities in richness (Spearman $\rho = 0.42$, $p = 1.3 \times 10^{-9}$, **Figure 2a**), evenness (Spearman $\rho = 0.24$, $p = 5.7 \times 10^{-4}$, **Figure 2b**).

As the bacterial and viral populations did not equally decrease in richness and evenness, they also did not equally correlate with MetS clinical parameters. Rather, viral richness was significantly negatively correlated with obesity, blood glucose levels, blood pressure, and triglyceride concentrations but bacterial richness was not ($p < 0.05$, **Figure 2c**). Bacterial evenness, meanwhile, did significantly negatively correlate with these clinical parameters while viral evenness did not ($p < 0.05$, **Figure 2d**). Increasingly severe MetS phenotypes thus result in stronger decreases in bacterial evenness than richness, while viral populations exhibit stronger decreases in richness than evenness. Decreasing bacterial evenness is likely because certain bacterial species are depleted in MetS, which results in the viruses infecting these depleted

bacteria to become undetectable, thereby decreasing richness more than evenness. Combined with the results showing MetS-associated reduction in viral abundance but no increase in lysogeny (**Supplementary Figure 2**), our findings indicate that certain phages are either completely removed from the gut or become too rare to detect in MetS.

Phages infecting select bacterial families are more abundant in MetS viromes

After showing that viral and bacterial populations mirror each other in MetS, we studied individual bacterial lineages and the phages that infect them. To do this, we first linked VCs to their bacterial hosts through CRISPR protospacer alignments, taxonomical classifications of bacterial sequences containing prophages, and VCs that contained previously isolated phages with known hosts (see methods for details). This resulted in 2,621 host predictions between 2,575 VCs (18% of all VCs) and eleven bacterial phyla, most commonly *Firmicutes* (2,067 VCs), *Bacteroidetes* (234 VCs), *Actinobacteria* (183 VCs) and *Proteobacteria* (94 VCs, **Supplementary Table 3**). Almost all VCs (2,532) were linked to one host phylum, though a notable minority of 43 VCs exhibited very wide predicted host ranges that spanned two or three phyla. This agrees with previously published estimates of cross-phyla phage host range[27].

For two thirds of VCs with host predictions (1,731), we could classify the host to the family level. To allow for more accurate statistical analysis, we selected the twelve most commonly occurring host families, which left 1,744 host predictions to 1,514 VCs (10.6% of all VCs). We then performed an analysis of compositions of microbiomes with bias correction (ANCOM-BC)[28], which showed that *Bacteroidaceae* VCs were more abundant in MetS viromes ($q = 2.2 \times 10^{-4}$) and *Ruminococcaceae* VCs ($q = 9.1 \times 10^{-3}$) in controls (**Figure 3a**).

ANCOM-BC on 16s rRNA gene sequencing data also identified *Bacteroidaceae* bacteria as significantly differentially abundant among MetS participants ($q = 1.03 \times 10^{-13}$). Since members of the widespread crAss-like gut phages infect *Bacteroidaceae* hosts[29,30], we ascertained whether this phage family was more abundant among MetS participants. We did not find significant relations between crAss-like phage abundance and MetS (**Supplementary Figure 4a**), although this phage family was present somewhat more often among control (70/99) than MetS (57/97) participants (Fisher's exact test, $p = 0.1$, **Supplementary Figure 4b**). In addition to being absent more often,

the participant with the highest relative abundance of crAss-like phages belonged to the MetS group (17.2% of total viral abundance, **Supplementary Figure 4a**), which was indicative of greater variation in crAss-like phage abundance among MetS (mean 1.29±2.62%) than controls (mean 0.830±1.44%). MetS-associated alterations to this widespread phage family may thus occur at an individual level.

Ruminococcaeae phages were significantly more abundant in healthy controls, in line with their host bacteria being commonly linked to healthy gut microbiomes[3,31,32]. Indeed, though correlations were absent at the family level, individual *Ruminococcaeae* ASVs were positively correlated with controls (**Supplementary Figure 5**). Corresponding examination of VCs of which we identified the host species showed control participants were significantly more abundant in VCs infecting *Faecalibacterium sp. CAG:74*, *Ruthenibacterium lactatiformans,* and *Subdoligranulum sp. APC924/74* (Wilcoxon signed rank test with Benjamini and Hochberg adjustment, $q \leq 0.05$, **Figure 3b**). These results are congruent with the population level data and suggest that phage occurrence and abundance in MetS gut microbiomes mostly corresponds with that of their hosts.

<u>*Bacteroidaceae* VCs are markers of the MetS phageome</u>

The above results all indicate that MetS gut viromes are distinct from those in healthy individuals. In light of this, we surveyed our cohort for individual VCs that were correlated with either MetS or healthy control viromes. ANCOM-BC uncovered nine VCs that were more abundant in MetS participants, and nine more in controls ($q \leq 0.05$, **Figure 4a**).

In line with the above findings that *Bacteroidaceae* phages are hallmarks of the MetS virome, three MetS-associated VCs infected *Bacteroides* bacteria. The first (VC_1180_0) contained a non-prophage contig (*i.e.*, no detected bacterial contamination) of 34,170 bp with a checkV[33] completion score of 100%. It further co-clustered with a contig that checkV identified as a complete prophage flanked by bacterial genes. Analysis with the contig annotation tool (CAT[34]) identified this contig as *Bacteroides fragilis*. Additionally, the most complete VC_1180_0 contig shared 6/69 (8.7%) ORFs with *Bacteroides uniformis Siphoviridae* phage Bacuni_F1[35] (BLASTp bit-score ≥ 50). The second MetS-associated *Bacteroides* VC (VC_786_0) contained one contig with CRISPR spacer hits to *Bacteroides*. Its most complete contig had a

CheckV completeness score of 98.94% and was classified by the contig annotation tool (CAT[34]) as *Phocaeicola vulgatus* (formerly *Bacteroides vulgatus*[36]). This near-complete contig furthermore shares 11/77 ORFs (14.3%) with *Riemerella Siphoviridae* phage RAP44 (BLASTp bit scores >50). This last finding was notable because the third and final MetS-associated *Bacteroides* VC (VC_775_1) also contained a near-complete genome (CheckV: 90.32% complete) that shared 16/81 ORFs (19.8%) with RAP44. Comparison of the most complete VC_786_0 and VC_775_1 contigs indicated that they share nine ORFs, revealing that they are part of an extended family of *Bacteroidetes Siphoviridae* phages of which members are hallmarks of MetS.

<u>A widespread phage family contains markers for healthy and MetS viromes</u>

Besides the above-mentioned *Bacteroidaceae* VCs, all other differentially abundant VCs with host links, two MetS- and four control-associated, infected *Firmicutes*, particularly in the *Clostridiales* order. The sole exception to this (VC_745_0) remarkably had CRISPR protospacer matches to *Firmicutes* bacteria *Faecalibacterium sp.* CAG: 74_58_120 and *Ruthenibacterium lactatiformans,* as well as to *Actinobacteria* bacterium *Parascardovia denticolens*. As this VC included genome fragments with simultaneous CRISPR protospacer hits to both phyla, VC_745_0 seemingly contains phages with an extraordinarily broad host range.

Besides this broad host range phage, our attention was drawn to the two MetS-associated *Clostridiales* VCs. Both were predicted to infect hosts that are usually associated with healthy gut microbiomes: *Roseburia*[3] for VC_659_0, and *Oscillospiraceae*[37] and *Faecalibacterium prausnitzii*[38] for VC_1040_0. Further examination of their largest genomes revealed that MetS-associated VC_659_0 was remarkably similar to two VCs that were significantly associated with healthy controls: the above-mentioned broad host-range VC_745_0 and the less broad host-range *Oscillibacter/Ruminococcaceae* VC_643_0 (**Figure 4b**).

Intrigued by this apparent relatedness of phages that included markers of MetS and healthy controls among our cohort, we sought to identify additional related phages among our cohort. For this we first determined the exact length of VC_659_0 genomes by analyzing read coverage plots of a prophage flanked by bacterial genes (**Figure 4b**). By analyzing coverage of the contig in subjects where bacterial genes were highly abundant but viral genes were absent, we extracted a genome of 68,665 bp long.

Homology searches of all 74 ORFs encoded by this prophage against all ORFs from all phage contigs in the cohort identified 249 contigs of over 30,000 bp that all shared nine genes (BLASTp bit score ≥ 50, **Figure 4b**). Additionally, we identified 51 *Siphoviridae* phage genomes in the National Center for Biotechnology Information (NCBI) nucleotide database that also shared these nine genes. With one exception, these were *Streptococcus* phages, the exception being *Erysipelothrix* phage phi1605.

The genes shared by all these phage genomes formed three categories. First are genes encoding structural functions: a major capsid protein, portal protein, CLP-like prohead maturation protease, and terminase. The second group are transcription-related genes encoding a DNA polymerase I, probable helicase, and nuclease. Finally, there are two genes that encode domains of unknown function, but which given their adjacency to the second group are likely transcription-related.

Earlier studies have used a cutoff of 10% gene similarity for phages that are in the same families, 20% for sub-families, and 40% for genera[39,40]. The nine shared genes form 10-25% of ORFs found on both the characterized phages and non-provirus contigs with checkV 'high-quality' designations. Thus, these phages form a family, which we dubbed the *Candidatus Heliusviridae*. Next, we further studied the *Ca. Heliusviridae* interrelatedness by calculating the pairwise percentages of shared protein clusters and hierarchically clustering the results (**Figure 5a**. This showed that the *Ca. Heliusviridae* form six groups, which we designated as *Ca. Heliusviridae* group alpha, beta, gamma, delta, epsilon, and zeta *Heliusvirinae*. A concatenated phylogenetic tree made from alignments of nine conserved *Ca. Heliusviridae* genes largely confirmed the hierarchical clustering (**Supplementary Figure 6**).

The *Ca. Heliusviridae* group alpha solely contained previously isolated *Streptococcus* phages, which both in the hierarchical clustering and the phylogenetic tree were distinct from the other genomes. Meanwhile, all three VCs that were significantly associated with either MetS or healthy controls where part of the *Ca. Heliusviridae* group zeta, by far the largest and most diverse group. Two of these, VC_659_0 and VC_745_0, formed distinct sub-clades in both hierarchical clustering and phylogenetic tree, while VC_643_0 conversely was spread out over multiple clades.

The *Ca. Heliusviridae* were present in 181 participants (92.3%), 94 controls and 87 MetS participants (**Figure 5b**). Of the *Heliusviridae* groups, the zeta was by far the most abundant, being present in 88 controls and 72 MetS participants. This meant

healthy control viromes were significantly more likely to contain *Heliusviridae* group zeta (Fisher exact test, $p = 0.0096$), though they were not significantly more abundant. Of the other candidate sub-families, the groups delta and epsilon were in significantly higher abundance (Wilcoxon signed rank test, $p = 0.0043$ and 0.0063, respectively) among MetS participants. The *Ca. Heliusviridae* group delta infects *Lachnospiraceae*, in particular *Butyrivibrio* sp. CAG:318 and *Lachnoclostridium* sp. An181. Meanwhile, the *Heliusviridae* group epsilon were distinct among the *Heliusviridae* in that they infect *Negativicutes* rather than *Clostridia*, specifically *Acidominacoccus* and several other genera in the *Veillonellaceae* (**Supplementary Table 3**). These results, combined with the fact that group zeta VC_659_0 is strongly correlated with MetS (**Figure 4a**), show that Ca. *Heliusviridae* are part of the core human gut virome, where they may affect intricate relations with human health.

<u>MetS-associated group zeta *Ca. Heliusviridae* prophages encode possible metabolic genes</u>

The *Ca. Heliusviridae* are generally linked to bacteria that are associated with healthy human gut microbiomes. Therefore, it is an apparent contradiction that MetS-associated *Ca. Heliusviridae* group zeta VC_659_0 infected *Roseburia*, a short chain fatty acids producer that is often abundant in healthy microbiomes[41]. Due to this contradiction, we explored this VC further. It contained two additional prophages, which where both incomplete (**Figure 6a**). Whole genome alignment showed that all three prophages shared their phage genes, and that the two incomplete ones also shared host-derived genes. This indicated that the incomplete prophages integrated into highly similar host bacteria which were distinct from *Roseburia*. To confirm this, we performed homology searches of the bacterial host ORFs found on these contigs against the NCBI nr database (BLASTp, bit-score ≥50). In both incomplete prophages, the majority of ORFs had *Blautia* as their top hit, which for a plurality of ORFs involved *Blautia wexlerae* (**Figure 6a**). VC_659_0 thus contains MetS-associated phages that integrate into at least two genera (*Roseburia* and *Blautia*) within the *Lachnospiraceae*.

To examine if the hosts infected by VC_659_0 were more abundant in MetS participants, we determined mean coverage of bacterial genes found adjacent to the prophages. This showed that both the *Blautia* and the *Roseburia* host genes were more abundant among MetS participants (Wilcoxon signed rank test, *Blautia* $p = 5.1 \times 10^{-4}$,

Roseburia $p = 0.042$, **Figure 6b** and **c**). The specific *Lachnospiraceae* strains infected by VC_659_0 phages thus seem to thrive in MetS microbiomes. This could in part be due to functions conferred upon these bacteria by these prophages, as particularly the *Roseburia* prophage which carried several virulence and metabolism-related genes, including ones encoding a chloramphenicol acetyltransferase 3 (2.3.1.28), Glyoxalase/Bleomycin resistance protein (IPR004360), multi antimicrobial extrusion protein (IPR002528), 2-succinyl-6-hydroxy-2,4-cyclohexadiene-1-carboxylate synthase (4.2.99.20), and NADPH-dependent FMN reductase (PF03358). The latter two in particular are both associated with vitamin K (menaquinone) metabolism, which is part of (an)aerobic respiration in bacteria[42]. This opens up the possibility that this *Roseburia* prophage aids its host bacterium, which in turn may contribute to MetS phenotypes.

Discussion

This is the first study of the gut virome in the context of MetS, a widespread global health concern. We have shown that MetS is associated with a general depletion of gut virus communities. This depletion mirrors bacterial populations, which is in agreement with recently reported direct correlations between gut viral and bacterial populations in healthy individuals[43]. The main driver of these effects is likely diet, which affects bacterial[44–46] as well as viral[47] populations. However, viral population depletions such as those we found may further exacerbate bacterial diversity losses, as low phage abundance may decrease their positive effects on bacterial diversity[48,49].

Like other studies, we found highly individual-specific[25,50] human gut viromes in which singular widespread phages are rare[14,15]. Despite the universally high inter-individual virome diversity, we found larger within-group variation among MetS viromes than healthy controls. This is consistent with the Anna Karenina principle (AKP), which holds that “all healthy microbiomes are similar; each dysbiotic microbiome is dysbiotic in its own way”[51]. Such AKP-dynamics mirror previous findings of obesity-related alterations in the gut bacterial populations[52]. Particularly, we hypothesize that stressors inherent to MetS perturb gut bacterial populations in a stochastic fashion, the effects of which reverberate to the viral populations and result in their increased within-group variation.

We further found strong negative correlations between the risk factors that constitute MetS and viral richness but not evenness. This likely results from the whole-genome sequencing approach that we took, which better captures phages inside bacterial cells (*e.g.*, actively replicating or integrated prophages) than transient phages from the envrionment[14]. The viral richness that we report here thus represent the number of species that are actively engaging with their hosts, while phages of which the bacterial host is depleted in number are more likely to be transient and thus less likely to be sequenced. This results in our findings that viral richness is lowered among the MetS group but evenness is not, which in turn gives the strong negative correlations between richness and MetS risk factors. It could also be that bacteria depleted in MetS reside in phage-inaccessible locales within the gut[53], which perhaps results in removal of the corresponding phages from the gut to below detectable levels. This would explain the stronger correlation between bacterial evenness than richness to MetS risk factors.

As most (gut) phages remain unstudied[14,54], it is often difficult to link phages to host bacteria[55]. Here, we linked roughly one tenth of all VCs to a bacterial host. The remaining majority of VCs likely represent phages that infect bacterial lineages lacking CRISPR systems[56], are exclusively lytic, or that integrate into hosts which we could not taxonomically classify. Whichever is the case, our study underscores the great need for methods that link phages to hosts with high accuracy[57,58]. From the phage-host linkages that we obtained, we found that phages infecting specific bacterial families tend to be either depleted (*Bifidobacteriaceae, Ruminococcaceae*, and *Oscillospiraceae)* or enriched (*Bacteroidaceae*) in tandem to their hosts. For the *Bifidobacteriaceae* and *Oscillospiracaeae*, this is in line with established studies that show depletion of these families in MetS[3] and MetS-associated disease states[31,37].

For *Ruminococcaceae* bacteria, associations with MetS and MetS-related diseases are less clear, with reports of both positive[3,32] or negative[38,59] associations. The specific *Ruminococcaceae* of which we link the phages to healthy controls, most notably *Faecalibacterium prausnitzii* and *Ruthenibacterium lactatiformans*, are both considered hallmarks of healthy human gut microbiomes[3,31,38]. Interestingly, we also succeeded in linking specific viral clusters that infect *Faecalibacterium* to both healthy controls (VC_745_0) and MetS participant groups (VC_1040_0). This contradiction may indicate that infections of *Faecalibacteria* may result in differing outcomes for the bacterium depending on the phage species. As both VCs contain integrase-like genes,

they represent temperate phages. It could be that VC_745_0 prophages augment *Faecalibacterium* growth, as prophages are known to do[60]. Meanwhile VC_1040_0 prophages could be detrimental to the same bacteria, for example by becoming lytic in the presence of MetS-associated dietary components, likewise to *Lactobacillus reuteri* prophages lysing their hosts in the presence of dietary fructose[9]. Such behavior can lead to the collapse of the bacterial population[41], and may thereby be a contributing factor to depletion of *Faecalibacterium* in MetS.

As mentioned, the *Bacteroidaceae* were the only bacterial family that are infected by phages which were significantly more abundant among MetS participants. Concordantly, we found several individual *Bacteroides* VCs that were MetS-associated. The *Bacteroides* are often positively associated with high-fat and high-protein diets[61,62]. Simultaneously, however, reports disagree on individual *Bacteroides* species and their associations with MetS-related diseases like obesity, type 2 diabetes, and non-alcoholic fatty liver disease[31]. Such conflicting reports likely reflect the large diversity in metabolic effects at strain level among these bacteria[63]. Based on our results, we drew two conclusions. First, that *Bacteroidaceae*-linked VCs mirror their hosts in MetS-associated abundance increase, and second that *Bacteroidaceae*-linked VCs are of significant interest to studies of the MetS microbiome. The latter conclusion is strengthened by findings that *Bacteroides* prophages can alter bacterial metabolism in the gut[8].

While *Bacteroidaceae* phages at large were thus seemingly associated with MetS phenotypes, we uncovered larger variation of crAss-like phage abundance, which suggest at individual-specific alterations to this gut phage family among MetS viromes. This widespread and often abundant human gut phage family infects *Bacteroidetes*, including members of the *Bacteroidaceae*[64,65]. As these phages are commonly linked to healthy gut microbiomes[40,65,66], it is conceivable that they would be negatively correlated with MetS viromes. That this is not the case among the entire cohort is likely due to the great variety within this family[65], and perhaps additionally to the hypothesized aptitude of crAss-like phages for host switching through genomic recombination[65].

Finally, our study revealed the *Candidatus Heliusviridae*, a highly widespread family of gut phages that largely infect *Clostridiales* hosts. This prospective family is also expansive, and includes at least six distinct candidate subfamilies. Our uncovering

of this novel human gut phage family underscores the usefulness of database-independent *de novo* sequence analyses[24,26,67], as well as the need for a wider view on viral taxonomy than has presently been exhibited in the field of gut viromics.

The *Ca. Heliusviridae* are of particular interest to studies of MetS and related illnesses because its member phages include some associated with MetS and others with healthy controls. Most striking is the fact that most of the bacteria infected by MetS-associated *Ca. Heliusviridae*, are generally producers of short chain fatty acids such as butyrate and commonly depleted in MetS[31]. The exception to this are the *Veillonellaceae* that are infected by the *Heliusviridae* group epsilon, which are found at elevated abundance in non-alcoholic fatty liver disease[31]. While higher abundance of some of the other butyrate-producers infected by *Ca. Heliusviridae* is associated with metformin use[68], this is used to treat type 2 diabetes rather than MetS. Furthermore, particularly in the case of *Roseburia/Blautia* VC_659_0, the bacteria and phages were both found at significantly higher levels among MetS. This thus rules out the possibility that these are phages that lyse their hosts in great number in the MetS virome. A possible explanation is that these phages are the causative agent behind the paradoxically elevated abundance of these normally beneficial bacteria. It could be that integration of *Ca. Heliusviridae* into their hosts alters the behavior of the bacteria to an extend that they become detrimental to health. This could be achieved with phage-encoded auxiliary genes, an occurrence known from marine viruses[69,70]. Alternatively, the location of integration on the bacterial genome can alter its behaviour[8].

As a result of this study, we hope that increasing research will be devoted to the virome and its role in MetS. This particularly extends to gaining a deeper understanding at the level of specific phage lineages such as the *Ca. Heliusviridae* and their hosts. Isolation of these phages, further refinement of their phylogeny, and study of their effect on their hosts could yield novel phage-based means by which gut dysbiosis can be studied.

Acknowledgements

PAdJ and TPMS were supported by a Senior Fellowship of the Dutch Diabetes Research Foundation (2019.82.004) to HH. KW was supported by a Novo Nordisk Foundation CAMIT grant 2018 to MN. BED was supported by the Netherlands Organization for Scientific Research (NWO) Vidi grant 864.14.004 and European Research Council (ERC) Consolidator grant 865694: DiversiPHI. The funders had no

role in the study design, the collection, analysis, and interpretation of data, the writing of the report, and the decision to submit the article for publication.

The HELIUS study is conducted by the Amsterdam UMC, location AMC with the Public Health Service of Amsterdam. Both provided core financial support for HELIUS. The HELIUS study is also funded by research grants of the Dutch Heart Foundation (Hartstichting; 2010T084), the Netherlands Organization for Health Research and Development (ZonMw; 200500003), the European Integration Fund (EIF; 2013EIF013), and the European Union (Seventh Framework Programme, FP-7; 278901). We gratefully acknowledge the AMC Biobank for their support in biobank management and high-quality storage of collected samples. We are most grateful to the participants of the HELIUS study and the management team, research nurses, interviewers, research assistants and other staff who have taken part in gathering the data of this study.

Author contributions

PAdJ and KW conducted data analysis; TPMS, BJvdB, AHZ, FLN, BED, and MN assisted with experimental design and data interpretation; PAdJ and HH designed the study and wrote the manuscript. All authors read and provided input on the manuscript.

Declaration of Interests

MN owns stock in, consults for, and has intellectual property rights in Caelus Health. He consults for Kaleido. None of these are directly relevant to the current paper.

Methods

Sequencing and contig assembly

The Healthy Life in an Urban Setting (HELIUS) cohort includes some 25,000 ethnically diverse participants from Amsterdam, the Netherlands. The cohort details were published previously[71]. The HELIUS cohort conformed to all relevant ethical considerations. It complied with the Declaration of Helsinki (6th, 7th revisions), and was approved by the Amsterdam University Medical Centers Medical Ethics Committee.

For details on stool sample collection from among the participants, their storage, and DNA extraction, see Deschasaux, *et al*[23]. Libraries for shotgun metagenomic sequencing were prepared using a PCR-free method at Novogene (Nanjing, China) on a HiSeq instrument (Illumina Inc. San Diego, CA, USA) with 150 bp paired-end reads and 6 Gb data/sample. All bioinformatics software was run using standard settings, unless otherwise stated. All sequencing reads are available at the European Nucleotide Archive under project PRJEB42542. Samples have accession numbers ERS5585222-ERS5585321, all viral contigs are under accession number ERZ1762427.

Following previously set definitions[72], participants were classified in the MetS group if three of the following five health issues occurred: abdominal obesity measured by waist circumference, insulin resistance measured by elevated fasting blood glucose, hypertriglyceridemia, low serum high-density lipoprotein (HDL), and high blood pressure[72].

Analysis of sequencing output started with assembly of the sequencing reads per sample (*i.e.,* 196 individual assemblies) into contigs using the metaSPAdes v3.14.1 software[73]. For each sample, we selected contigs of more than 5,000 bp for further analysis. In addition, among contigs between 1,500 and 5,000 bp we identified circular contigs by checking for identical terminal ends using a custom R script that employed the Biostrings R package v3.12[74]. All 6,780,412 circular contigs and contigs over 5,000 bp were then pooled before viral sequence prediction.

<u>Viral and bacterial sequence selection</u>

We predicted viral sequences as described previously[75]. In short, we first analyzed contigs using VirSorter v1.0.6[76] and selected those in category 1, 2, 4, and 5. In parallel, contigs were analyzed using VirFinder v1.1, after which we selected those with a score above 0.9 and a p-value below 0.05. We additionally classified contigs as viral if (I) they were both in VirSorter categories 3 or 6 and had VirFinder scores above 0.7 with p-values below 0.05, and (II) annotation with the contig annotation tool (CAT) v5.1.2[34] was as “Viruses” or “unclassified” at the superkingdom level. After removing those with CAT classifications as Eukaryotic viruses, this resulted in a database of 45,568 viral contigs. Bacterial sequences were predicted by selecting all contigs that CAT annotated in the “Bacteria” at the superkingdom level, and removing contigs that

were also found in the viral dataset. An exception was made for prophage contigs in VirSorter category 4, 5, and 6, which were left among the bacterial dataset (see "Phage-host linkage prediction"). This resulted in a total of 1,579,361 bacterial contigs. The 1,624,929 bacterial and viral datasets were then concatenated and deduplicated using dedupe from BBTools v38.84 with a minimal identity cutoff of 90% (option minidentity=90). This identified 759,403 duplicates and resulted in 829,633 non-redundant bacterial sequences and 25,893 non-redundant viral sequences. While the bacterial sequences were used for host prediction (see "Phage-host linkage prediction"), we subsequently predicted open reading frames (ORFs) in viral contigs using Prodigal v2.6.2[77] (option -p meta). These ORFs were then used to group viral sequences in viral clusters (VCs) using vContact2 v0.9.18[24]. This resulted in 2,866 VCs comprising 14,434 viral contigs and 11,460 singletons and outliers, which we treated as VCs with one member. This resulted in 14,326 VCs. For a full accounting of viral contigs, see **Supplementary Table 2 and 4.**

Read mapping and community composition

For bacterial community composition, we used sequencing data targeting the V4 region of the 16s rRNA gene that had been performed previously[23]. This previous publication also included bacterial community composition analyses for these samples, of which the methodological details can be found in Deschasaux, *et al*[23].

To determine viral community composition, we mapped reads from each sample to the non-redundant contig dataset using bowtie2 v2.4.0[78]. As previously recommended[26], we removed spurious read mappings at less than 90% identity using coverM filter v0.5.0 (unpublished; https://github.com/wwood/CoverM, option -min-read-percent-identity 90). The number of reads per contig was calculated using samtools idxstats v1.10[79]. As was also recommended[26], contig coverage was calculated with bedtools genomecov v2.29.2[80], and read counts to contigs with a coverage of less than 75% were set to zero. Read counts for each sample were finally summed per VC. All contigs were analyzed for completion with CheckV v 0.7.0-1[33].

Ecological measures

In all boxplots, we tested statistical significance using the Wilcoxon rank sum test as it is implemented in the ggpubr v0.4.0 R package (available from: https://cran.r-project.org/web/packages/ggpubr/index.html). Unless stated otherwise, all plots were made using either ggpubr or the ggplot2 v3.3.2 R package (available from: https://cran.r-project.org/web/packages/ggplot2/index.html). Alpha diversity measures (observed VCs and Shannon H' for phages and Chao1 and Shannon H' for bacteria) were calculated using read count tables with the plot_richness function in the phyloseq R package v1.33.0[81]. For β-diversity, we converted read counts to relative abundances using the transform function from the microbiome v1.11.2 R package. We then used the phyloseq package to calculate pairwise Bray-Curtis dissimilarities and construct a principal coordinates analysis (PCoA). Statistical significance of separation in the PCoA analysis was determined with a permutational multivariate analysis of variance (permanova) using the adonis function from the vegan R package[82]. Direct correlation coefficients between richness and diversity were calculated using the stat_cor function in the ggpubr R package.

Phage-host linkage prediction

We predicted VC-bacterium links in three ways: (i) CRISPR protospacers, (ii) prophage similarity, and (iii) characterized phage similarity.

We predicted CRISPR arrays among the bacterial contigs using CRISPRdetect v2.4[83] (option array_quality_score_cutoff 3) and used these to match bacterial contigs and viral contigs. In addition, we used a dataset of 1,473,418 CRISPR spacers that had previously been predicted[58,84] in genomes contained in the Pathosystems Resource Integration Center (PATRIC)[85] to match to viral contigs with spacePharer v2-fc5e668[86] using standard settings and cutoffs. This process resulted in 3,727 spacer hits, of which 2,244 hits were either to PATRIC genomes or to bacterial contigs from this study with definite CAT classifications at the phylum level (**Supplementary Table 3**).

To identify predicted viral contigs with high sequence similarity to prophages, we analyzed which viral clusters contained on of the 7,691 bacterial contigs with VirSorter prophage predictions in category 4 or 5. CAT was subsequently used to determine the taxonomy of bacterial contigs with prophage regions. In total, we linked 1,102 VCs to prophages with this approach.

Finally, VCs were linked to bacterial hosts by vContact2 clustering with characterized phages from the viral RefSeq V85 database[87] with a known host. To achieve this, we selected all VCs from the vContact2 output that contained both characterized genomes and viral contigs. If all characterized phages infected hosts within the same bacterial family, we took that to mean that the whole VC infects hosts from that family. This approach linked 44 VCs to hosts.

Differential abundance analysis

To determine which bacteria and VCs were differentially abundant between MetS and control subjects, we employed the analysis of composition of microbiomes with bias correction (ANCOM-BC)[28]. This novel method, unlike other similar methods like DeSeq2, takes into account the compositional nature of metagenomics sequencing data[88]. To implement this method, we applied the ANCOM-BC v1.0.2 R package to raw read count tables, as ANCOM-BC employs internal corrections for library size and sampling biases[28]. Significance cutoff was set at an adjusted p-value of 0.05, p-values were adjusted using the Holm–Bonferroni method, and all entities (bacteria taxa/VCs) that were present in more than 10% of the samples were included (options p_adj_method = "holm", zero_cut = 0.9, lib_cut = 0, struc_zero = T, neg_lb = F, tol = 1e-5, max_iter = 100, alpha = 0.05).

crAss-like phages

To identify crAss-like phages, we employed a methodology described earlier[40]. Shortly, a BLAST database was made containing all ORFs from all viral contigs (predicted before viral clustering, see “Viral and bacterial sequence selection”) using BLAST v2.9.0+[89]. We then performed two BLASTp searches in this database, one with the terminase (YP_009052554.1) and one with the polymerase (YP_009052497.1) of crAssphage (NC_024711.1), with a bitscore cutoff of 50. All viral contigs that had (i) a hit against both crAssphage terminase and polymerase and a query alignment of ≥350 bp, and (ii) a contig length of ≥70 kbp were considered crAss-like phages. This resulted in 146 crAss-like phage contigs, which were contained in 29 VCs.

Candidatus *Heliusviridae* analysis

To detect pairwise similarity, whole genome analyses were constructed with Easyfig v2.2.5[90]. The prophage borders in NODE_38_length_205884_cov_102.806990 were determined by determining the read depth along the entire contig from the bam files with read mapping data ("Read mapping and community composition") using bedtools genomecov v2.29.2[80] with option -bg. Resultant output was parsed and plotted in R. Other related phages among the cohort were detected by performing a BLASTp search with all viral ORFs of NODE_38_length_205884_cov_102.806990 against all viral ORFs of the cohort with Diamond v2.0.4. This identified nine genes that were present in 249 contigs. The ORFs on these contigs were annotated using PROKKA v[91]1.14.6 and InterProScan v5.48-83.0[92]. To identify isolated phages that share these nine contigs, we performed a BLASTp against the NCBI nr-database using the NCBI webserver[93] on February 26 2021 and collected all genomes with hits against all nine genes (bit score ≥50).

The phages sharing all nine genes were clustered by analyzing them with vContact2 v0.9.18[24], extracting the protein clustering data and calculating the number of shared clusters between each pair of contigs. Contigs were clustered in R based on Euclidean distances with the average agglomeration method.

To build a taxonomic tree, the nine genes were separately aligned using Clustal Omega v1.2.4[94], positions with more than 90% gaps were removed with trimAl v1.4.rev15[95] and alignments were concatenated. From the concatenated alignment, an unrooted phylogenetic tree was built using IQ- Tree v2.0.3[96] using model finder[97] and performing 1000 iterations of both SH-like approximate likelihood ratio test and the ultrafast bootstrap approximation (UFBoot)[98]. In addition, ten iterations of the tree were separately constructed, as has been recommended[99] (Zhou et al., 2018) (IQ-Tree options -bb 1000, -alrt 1000, and --runs 10).

References

1. Belkaid, Y. & Hand, T. W. Role of the microbiota in immunity and inflammation. *Cell* **157**, 121–141 (2014).
2. Rastelli, M., Cani, P. D. & Knauf, C. The Gut Microbiome Influences Host Endocrine Functions. *Endocr. Rev.* **40**, 1271–1284 (2019).
3. Gurung, M. *et al.* Role of gut microbiota in type 2 diabetes pathophysiology. *EBioMedicine* **51**, 102590 (2020).

4. Lang, S. & Schnabl, B. Microbiota and Fatty Liver Disease—the Known, the Unknown, and the Future. *Cell Host Microbe* **28**, 233–244 (2020).
5. Frank, D. N. *et al.* Molecular-phylogenetic characterization of microbial community imbalances in human inflammatory bowel diseases. *Proc. Natl. Acad. Sci.* **104**, 13780–13785 (2007).
6. Clooney, A. G. *et al.* Whole-Virome Analysis Sheds Light on Viral Dark Matter in Inflammatory Bowel Disease. *Cell Host Microbe* **26**, 764-778.e5 (2019).
7. Norman, J. M. *et al.* Disease-Specific Alterations in the Enteric Virome in Inflammatory Bowel Disease. *Cell* **160**, 447–460 (2015).
8. Campbell, D. E. *et al.* Infection with Bacteroides Phage BV01 Alters the Host Transcriptome and Bile Acid Metabolism in a Common Human Gut Microbe. *Cell Rep.* **32**, 108142 (2020).
9. Oh, J.-H. *et al.* Dietary Fructose and Microbiota-Derived Short-Chain Fatty Acids Promote Bacteriophage Production in the Gut Symbiont Lactobacillus reuteri. *Cell Host Microbe* **25**, 273-284.e6 (2019).
10. Reyes, A. *et al.* Gut DNA viromes of Malawian twins discordant for severe acute malnutrition. *Proc. Natl. Acad. Sci.* **112**, 11941–11946 (2015).
11. Ma, Y., You, X., Mai, G., Tokuyasu, T. & Liu, C. A human gut phage catalog correlates the gut phageome with type 2 diabetes. *Microbiome* **6**, 1–12 (2018).
12. De Sordi, L., Lourenço, M. & Debarbieux, L. The Battle Within: Interactions of Bacteriophages and Bacteria in the Gastrointestinal Tract. *Cell Host Microbe* **25**, 210–218 (2019).
13. Paez-Espino, D. *et al.* Uncovering Earth's virome. *Nature* **536**, 425–430 (2016).
14. Gregory, A. C. *et al.* The Gut Virome Database Reveals Age-Dependent Patterns of Virome Diversity in the Human Gut. *Cell Host Microbe* **28**, 724-740.e8 (2020).
15. Dutilh, B. E. *et al.* A highly abundant bacteriophage discovered in the unknown sequences of human faecal metagenomes. *Nat. Commun.* **5**, 4498 (2014).
16. Yutin, N. *et al.* Discovery of an expansive bacteriophage family that includes the most abundant viruses from the human gut. *Nat. Microbiol.* **3**, 38–46 (2018).
17. O'Neill, S. & O'Driscoll, L. Metabolic syndrome: A closer look at the growing epidemic and its associated pathologies. *Obes. Rev.* **16**, 1–12 (2015).
18. Dabke, K., Hendrick, G. & Devkota, S. The gut microbiome and metabolic syndrome. *J. Clin. Invest.* **129**, 4050–4057 (2019).

19. Mazidi, M., Rezaie, P., Kengne, A. P., Mobarhan, M. G. & Ferns, G. A. Gut microbiome and metabolic syndrome. *Diabetes Metab. Syndr. Clin. Res. Rev.* **10**, S150–S157 (2016).
20. Fujisaka, S. *et al.* Diet, Genetics, and the Gut Microbiome Drive Dynamic Changes in Plasma Metabolites. *Cell Rep.* **22**, 3072–3086 (2018).
21. Ussar, S. *et al.* Interactions between gut microbiota, host genetics and diet modulate the predisposition to obesity and metabolic syndrome. *Cell Metab.* **22**, 516–530 (2015).
22. Haro, C. *et al.* The gut microbial community in metabolic syndrome patients is modified by diet. *J. Nutr. Biochem.* **27**, 27–31 (2016).
23. Deschasaux, M. *et al.* Depicting the composition of gut microbiota in a population with varied ethnic origins but shared geography. *Nat. Med.* **24**, 1526–1531 (2018).
24. Bin Jang, H. *et al.* Taxonomic assignment of uncultivated prokaryotic virus genomes is enabled by gene-sharing networks. *Nat. Biotechnol.* **37**, 632–639 (2019).
25. Manrique, P. *et al.* Healthy human gut phageome. *Proc. Natl. Acad. Sci.* **113**, 10400–10405 (2016).
26. Roux, S., Emerson, J. B., Eloe-Fadrosh, E. A. & Sullivan, M. B. Benchmarking viromics: An in silico evaluation of metagenome-enabled estimates of viral community composition and diversity. *PeerJ* **2017**, 1–26 (2017).
27. Camarillo-Guerrero, L. F., Almeida, A., Rangel-Pineros, G., Finn, R. D. & Lawley, T. D. Massive expansion of human gut bacteriophage diversity. *Cell* **184**, 1098-1109.e9 (2021).
28. Lin, H. & Peddada, S. Das. Analysis of compositions of microbiomes with bias correction. *Nat. Commun.* **11**, 1–11 (2020).
29. Hryckowian, A. J. *et al.* Bacteroides thetaiotaomicron-Infecting Bacteriophage Isolates Inform Sequence-Based Host Range Predictions. *Cell Host Microbe* **28**, 371-379.e5 (2020).
30. Yutin, N. *et al.* Analysis of metagenome-assembled viral genomes from the human gut reveals diverse putative CrAss-like phages with unique genomic features. *Nat. Commun.* **12**, 1044 (2021).
31. Aron-Wisnewsky, J. *et al.* Gut microbiota and human NAFLD: disentangling microbial signatures from metabolic disorders. *Nat. Rev. Gastroenterol. Hepatol.*

17, 279–297 (2020).

32. Liu, R. *et al.* Gut microbiome and serum metabolome alterations in obesity and after weight-loss intervention. *Nat. Med.* **23**, 859–868 (2017).

33. Nayfach, S. *et al.* CheckV assesses the quality and completeness of metagenome-assembled viral genomes. *Nat. Biotechnol.* (2020). doi:10.1038/s41587-020-00774-7

34. Von Meijenfeldt, F. A. B., Arkhipova, K., Cambuy, D. D., Coutinho, F. H. & Dutilh, B. E. Robust taxonomic classification of uncharted microbial sequences and bins with CAT and BAT. *Genome Biol.* **20**, 1–14 (2019).

35. Hedzet, S., Accetto, T. & Rupnik, M. Lytic Bacteroides uniformis bacteriophages exhibiting host tropism congruent with diversity generating retroelement. *bioRxiv* 2020.10.09.334284 (2020). doi:10.1101/2020.10.09.334284

36. García-López, M. *et al.* Analysis of 1,000 Type-Strain Genomes Improves Taxonomic Classification of Bacteroidetes. *Front. Microbiol.* **10**, (2019).

37. Maya-Lucas, O. *et al.* The gut microbiome of Mexican children affected by obesity. *Anaerobe* **55**, 11–23 (2019).

38. Miquel, S. *et al.* Faecalibacterium prausnitzii and human intestinal health. *Curr. Opin. Microbiol.* **16**, 255–261 (2013).

39. Lavigne, R., Seto, D., Mahadevan, P., Ackermann, H. W. & Kropinski, A. M. Unifying classical and molecular taxonomic classification: analysis of the Podoviridae using BLASTP-based tools. *Res. Microbiol.* **159**, 406–414 (2008).

40. Guerin, E. *et al.* Biology and Taxonomy of crAss-like Bacteriophages, the Most Abundant Virus in the Human Gut. *Cell Host Microbe* **24**, 653-664.e6 (2018).

41. Cornuault, J. K. *et al.* The enemy from within: a prophage of Roseburia intestinalis systematically turns lytic in the mouse gut, driving bacterial adaptation by CRISPR spacer acquisition. *ISME J.* **14**, 771–787 (2020).

42. Walther, B., Karl, J. P., Booth, S. L. & Boyaval, P. Menaquinones, Bacteria, and the Food Supply: The Relevance of Dairy and Fermented Food Products to Vitamin K Requirements. *Adv. Nutr.* **4**, 463–473 (2013).

43. Moreno-Gallego, J. L. *et al.* Virome Diversity Correlates with Intestinal Microbiome Diversity in Adult Monozygotic Twins. *Cell Host Microbe* **25**, 261-272.e5 (2019).

44. Zmora, N., Suez, J. & Elinav, E. You are what you eat: diet, health and the gut microbiota. *Nat. Rev. Gastroenterol. Hepatol.* **16**, 35–56 (2019).

45. Falony, G. *et al.* Population-level analysis of gut microbiome variation. *Science (80-.).* **352**, 560–564 (2016).
46. Zhernakova, A. *et al.* Population-based metagenomics analysis reveals markers for gut microbiome composition and diversity. *Science (80-.).* **352**, 565–569 (2016).
47. Minot, S. *et al.* The human gut virome: Inter-individual variation and dynamic response to diet. *Genome Res.* **21**, 1616–1625 (2011).
48. Rodriguez-Valera, F. *et al.* Explaining microbial population genomics through phage predation. *Nat. Rev. Microbiol.* **7**, 828–836 (2009).
49. Koskella, B. & Brockhurst, M. A. Bacteria–phage coevolution as a driver of ecological and evolutionary processes in microbial communities. *FEMS Microbiol. Rev.* **38**, 916–931 (2014).
50. Shkoporov, A. N. *et al.* The Human Gut Virome Is Highly Diverse, Stable, and Individual Specific. *Cell Host Microbe* **26**, 527-541.e5 (2019).
51. Zaneveld, J. R., McMinds, R. & Vega Thurber, R. Stress and stability: applying the Anna Karenina principle to animal microbiomes. *Nat. Microbiol.* **2**, 17121 (2017).
52. Holmes, I., Harris, K. & Quince, C. Dirichlet Multinomial Mixtures: Generative Models for Microbial Metagenomics. *PLoS One* **7**, e30126 (2012).
53. Lourenço, M. *et al.* The Spatial Heterogeneity of the Gut Limits Predation and Fosters Coexistence of Bacteria and Bacteriophages. *Cell Host Microbe* **28**, 390-401.e5 (2020).
54. Hatfull, G. F. Dark Matter of the Biosphere: the Amazing World of Bacteriophage Diversity. *J. Virol.* **89**, 8107–8110 (2015).
55. Edwards, R. A., McNair, K., Faust, K., Raes, J. & Dutilh, B. E. Computational approaches to predict bacteriophage-host relationships. *FEMS Microbiol. Rev.* **40**, 258–272 (2016).
56. Burstein, D. *et al.* Major bacterial lineages are essentially devoid of CRISPR-Cas viral defence systems. *Nat. Commun.* **7**, 10613 (2016).
57. Džunková, M. *et al.* Defining the human gut host–phage network through single-cell viral tagging. *Nat. Microbiol.* **4**, 2192–2203 (2019).
58. de Jonge, P. A. *et al.* Adsorption Sequencing as a Rapid Method to Link Environmental Bacteriophages to Hosts. *iScience* **23**, 101439 (2020).
59. Walters, W. A., Xu, Z. & Knight, R. Meta-analyses of human gut microbes

associated with obesity and IBD. *FEBS Lett.* **588**, 4223–4233 (2014).

60. Drulis-Kawa, Z., Majkowska-Skrobek, G., Maciejewska, B., Delattre, A.-S. & Lavigne, R. Learning from Bacteriophages - Advantages and Limitations of Phage and Phage-Encoded Protein Applications. *Curr. Protein Pept. Sci.* **13**, 699–722 (2012).

61. Ridaura, V. K. *et al.* Gut Microbiota from Twins Discordant for Obesity Modulate Metabolism in Mice. *Science (80-.).* **341**, 1241214 (2013).

62. David, L. A. *et al.* Diet rapidly and reproducibly alters the human gut microbiome. *Nature* **505**, 559–563 (2014).

63. De Filippis, F. *et al.* Distinct Genetic and Functional Traits of Human Intestinal Prevotella copri Strains Are Associated with Different Habitual Diets. *Cell Host Microbe* **25**, 444-453.e3 (2019).

64. Shkoporov, A. N. *et al.* ΦCrAss001 represents the most abundant bacteriophage family in the human gut and infects Bacteroides intestinalis. *Nat. Commun.* **9**, 4781 (2018).

65. Koonin, E. V. & Yutin, N. The crAss-like Phage Group: How Metagenomics Reshaped the Human Virome. *Trends Microbiol.* **28**, 349–359 (2020).

66. Edwards, R. A. *et al.* Global phylogeography and ancient evolution of the widespread human gut virus crAssphage. *Nat. Microbiol.* **4**, 1727–1736 (2019).

67. Garmaeva, S. *et al.* Studying the gut virome in the metagenomic era: Challenges and perspectives. *BMC Biol.* **17**, 1–14 (2019).

68. De La Cuesta-Zuluaga, J. *et al.* Metformin is associated with higher relative abundance of mucin-degrading akkermansia muciniphila and several short-chain fatty acid-producing microbiota in the gut. *Diabetes Care* **40**, 54–62 (2017).

69. Gazitúa, M. C. *et al.* Potential virus-mediated nitrogen cycling in oxygen-depleted oceanic waters. *ISME J.* (2020). doi:10.1038/s41396-020-00825-6

70. Sharon, I. *et al.* Photosystem I gene cassettes are present in marine virus genomes. *Nature* **461**, 258–262 (2009).

71. Snijder, M. B. *et al.* Cohort profile: The Healthy Life in an Urban Setting (HELIUS) study in Amsterdam, the Netherlands. *BMJ Open* **7**, 1–11 (2017).

72. Alberti, K. G. M. M. *et al.* Harmonizing the metabolic syndrome: A joint interim statement of the international diabetes federation task force on epidemiology and prevention; National heart, lung, and blood institute; American heart association; World heart federation; International . *Circulation* **120**, 1640–1645 (2009).

73. Nurk, S., Meleshko, D., Korobeynikov, A. & Pevzner, P. A. MetaSPAdes: A new versatile metagenomic assembler. *Genome Res.* **27**, 824–834 (2017).
74. Pagès H, Aboyoun P, Gentleman R, D. S. Biostrings: Efficient manipulation of biological strings. (2020).
75. Gregory, A. C. *et al.* Marine DNA Viral Macro- and Microdiversity from Pole to Pole. *Cell* **177**, 1109-1123.e14 (2019).
76. Roux, S., Enault, F., Hurwitz, B. L. & Sullivan, M. B. VirSorter: mining viral signal from microbial genomic data. *PeerJ* **3**, e985 (2015).
77. Hyatt, D. *et al.* Prodigal: prokaryotic gene recognition and translation initiation site identification. *BMC Bioinformatics* **11**, 119 (2010).
78. Langmead, B. & Salzberg, S. L. Fast gapped-read alignment with Bowtie 2. *Nat. Methods* **9**, 357–359 (2012).
79. Li, H. *et al.* The Sequence Alignment/Map format and SAMtools. *Bioinformatics* **25**, 2078–2079 (2009).
80. Quinlan, A. R. *BEDTools: The Swiss-Army tool for genome feature analysis*. *Current Protocols in Bioinformatics* **2014**, (2014).
81. McMurdie, P. J. & Holmes, S. phyloseq: An R Package for Reproducible Interactive Analysis and Graphics of Microbiome Census Data. *PLoS One* **8**, e61217 (2013).
82. Dixon, P. VEGAN, a package of R functions for community ecology. *J. Veg. Sci.* **14**, 927–930 (2003).
83. Biswas, A., Staals, R. H. J., Morales, S. E., Fineran, P. C. & Brown, C. M. CRISPRDetect: A flexible algorithm to define CRISPR arrays. *BMC Genomics* **17**, 1–14 (2016).
84. Nobrega, F. L., Walinga, H., Dutilh, B. E. & Brouns, S. J. J. J. Prophages are associated with extensive CRISPR–Cas auto-immunity. *Nucleic Acids Res.* **48**, 12074–12084 (2020).
85. Wattam, A. R. *et al.* PATRIC, the bacterial bioinformatics database and analysis resource. *Nucleic Acids Res.* **42**, 581–591 (2014).
86. Zhang, R. *et al.* SpacePHARER: Sensitive identification of phages from CRISPR spacers in prokaryotic hosts. *bioRxiv* 2020.05.15.090266 (2020). doi:10.1101/2020.05.15.090266
87. Pruitt, K. D., Tatusova, T. & Maglott, D. R. NCBI reference sequences (RefSeq): A curated non-redundant sequence database of genomes, transcripts and

proteins. *Nucleic Acids Res.* **35**, 61–65 (2007).

88. Gloor, G. B., Macklaim, J. M., Pawlowsky-Glahn, V. & Egozcue, J. J. Microbiome datasets are compositional: And this is not optional. *Front. Microbiol.* **8**, 1–6 (2017).

89. Camacho, C. *et al.* BLAST+: architecture and applications. *BMC Bioinformatics* **10**, 421 (2009).

90. Sullivan, M. J., Petty, N. K. & Beatson, S. A. Easyfig: A genome comparison visualizer. *Bioinformatics* **27**, 1009–1010 (2011).

91. Seemann, T. Prokka: Rapid prokaryotic genome annotation. *Bioinformatics* **30**, 2068–2069 (2014).

92. Jones, P. *et al.* InterProScan 5: Genome-scale protein function classification. *Bioinformatics* **30**, 1236–1240 (2014).

93. Johnson, M. *et al.* NCBI BLAST: a better web interface. *Nucleic Acids Res.* **36**, 5–9 (2008).

94. Sievers, F. & Higgins, D. G. Clustal Omega for making accurate alignments of many protein sequences. *Protein Sci.* **27**, 135–145 (2018).

95. Capella-Gutiérrez, S., Silla-Martínez, J. M. & Gabaldón, T. trimAl: A tool for automated alignment trimming in large-scale phylogenetic analyses. *Bioinformatics* **25**, 1972–1973 (2009).

96. Nguyen, L. T., Schmidt, H. A., Von Haeseler, A. & Minh, B. Q. IQ-TREE: A fast and effective stochastic algorithm for estimating maximum-likelihood phylogenies. *Mol. Biol. Evol.* **32**, 268–274 (2015).

97. Kalyaanamoorthy, S., Minh, B. Q., Wong, T. K. F., von Haeseler, A. & Jermiin, L. S. ModelFinder: fast model selection for accurate phylogenetic estimates. *Nat. Methods* **14**, 587–589 (2017).

98. Hoang, D. T., Chernomor, O., von Haeseler, A., Minh, B. Q. & Vinh, L. S. UFBoot2: Improving the Ultrafast Bootstrap Approximation. Molecular biology and evolution. *Mol. Biol. Evol.* **35**, 518–522 (2018).

99. Zhou, X., Shen, X. X., Hittinger, C. T. & Rokas, A. Evaluating fast maximum likelihood-based phylogenetic programs using empirical phylogenomic data sets. *Mol. Biol. Evol.* **35**, 486–503 (2018).

100. Charrad, M., Ghazzali, N., Boiteau, V. & Niknafs, A. NbClust : An R Package for Determining the Relevant Number of Clusters in a Data Set. *J. Stat. Softw.* **61**, 11744–11750 (2014).

Figures

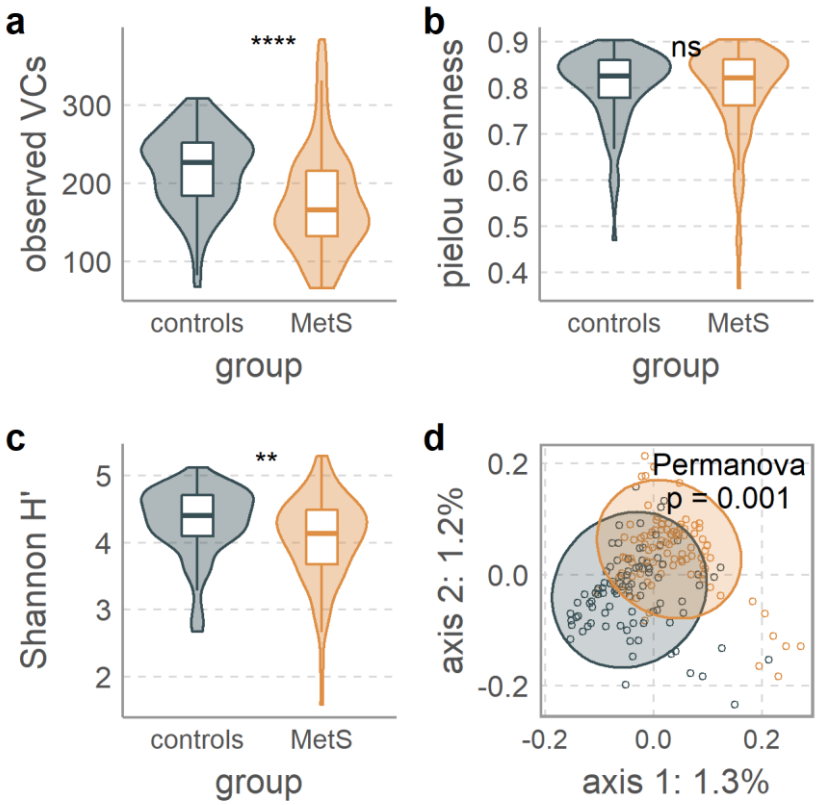

Figure 1: Gut virus populations are altered in MetS. a MetS-associated decreased viral species richness is evidenced by the number of unique VCs observed per sample. **b** No change in viral pielou evenness measurements. **c** significantly decreased viral α-diversity measured by Shannon diversity. **d** clear separation between viromes of MetS and control participant as shown by β-diversity depicted in a principal coordinates analysis (PCoA) of Bray-Curtis dissimilarities. Statistical significance in A-C is according to the Wilcoxon signed rank test, where p-values are denoted as follows: ns not significant, * ≤ 0.05, ** ≤ 0.01, *** ≤ 0.001, **** ≤ 0.0001.

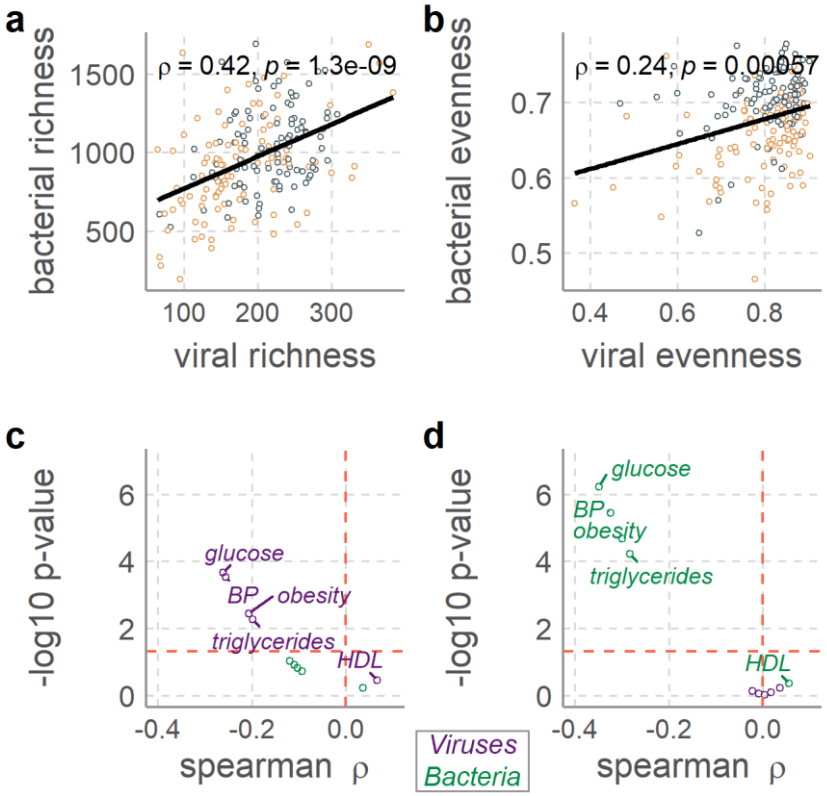

Figure 2: correlations between viral and bacterial populations as well as between population measures and MetS clinical parameters. Strong correlations between **a** viral richness (observed VCs) and bacterial richness (Chao1 index), as well as between **b** viral and bacterial evenness (Pielou's index), both with significant positive Spearman's rank correlation coefficient. Both of these measures were correlated to MetS clinical parameters. Plotted are the Spearman's rank correlation coefficients versus corresponding p-values of correlations between the five MetS risk factors and **c** richness and **d** evenness. Horizontal red lines denote p-values of 0.05.

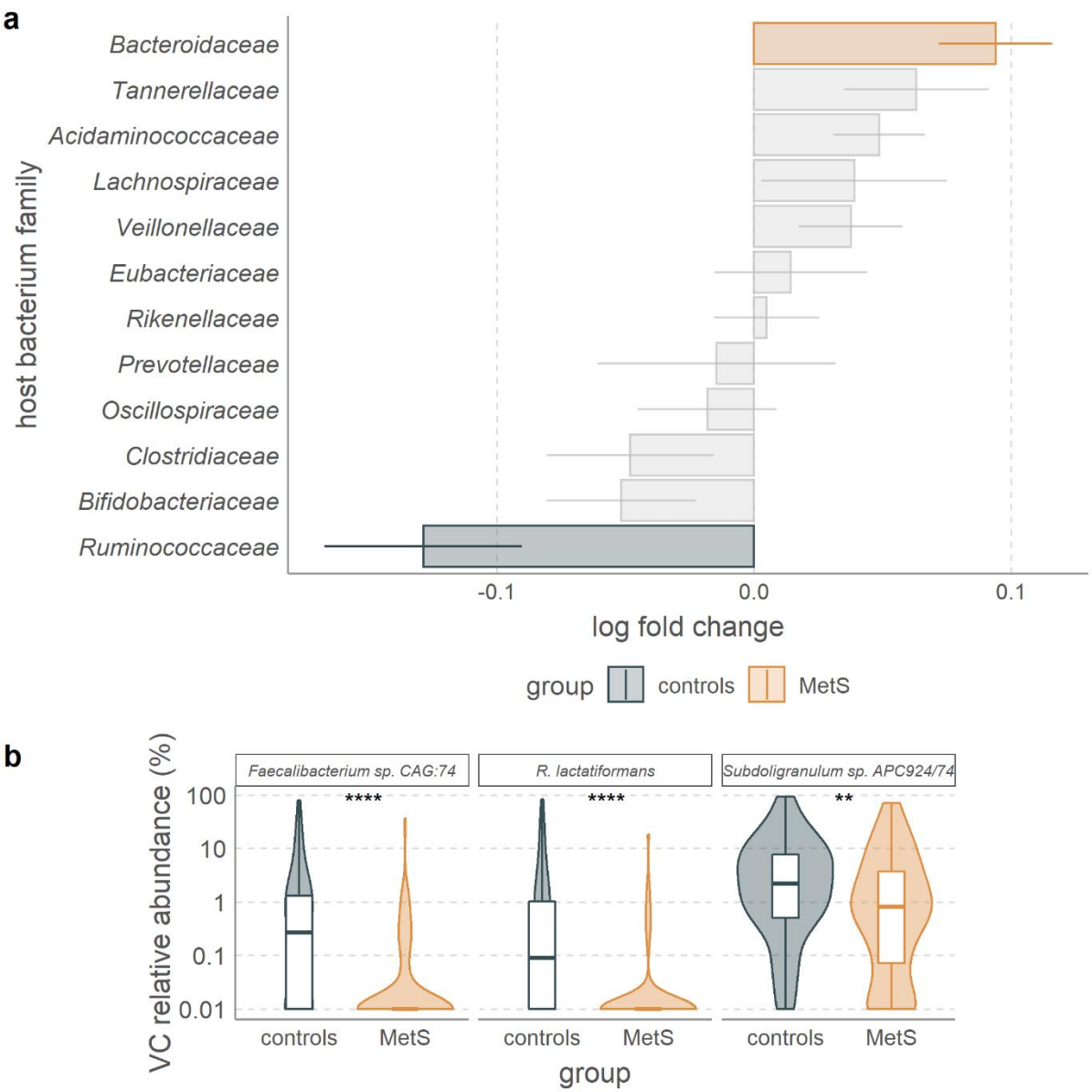

Figure 3: Phages infecting selected bacterial families are differentially abundant in MetS or healthy controls. a ANCOM-BC[28] analysis of VCs that infect the twelve bacterial families to which the most VCs were linked shows significant association of *Bacteroidaceae* VCs and MetS, as well as *Ruminococcaceae* VCs and healthy controls. **b** relative abundance comparisons between MetS and control participants of VCs infecting *Faecalibacterium sp.* CAG:74, *Ruthenibacterium lactatiformans*, *Subdoligranulum sp.* APC924/74. Stars denote significance according to the Wilcoxon signed rank test, with p-values adjusted with the Benjamini and Hochberg procedure (*q*). * ≤ 0.05, ** ≤ 0.01, *** ≤ 0.001, **** ≤ 0.0001.

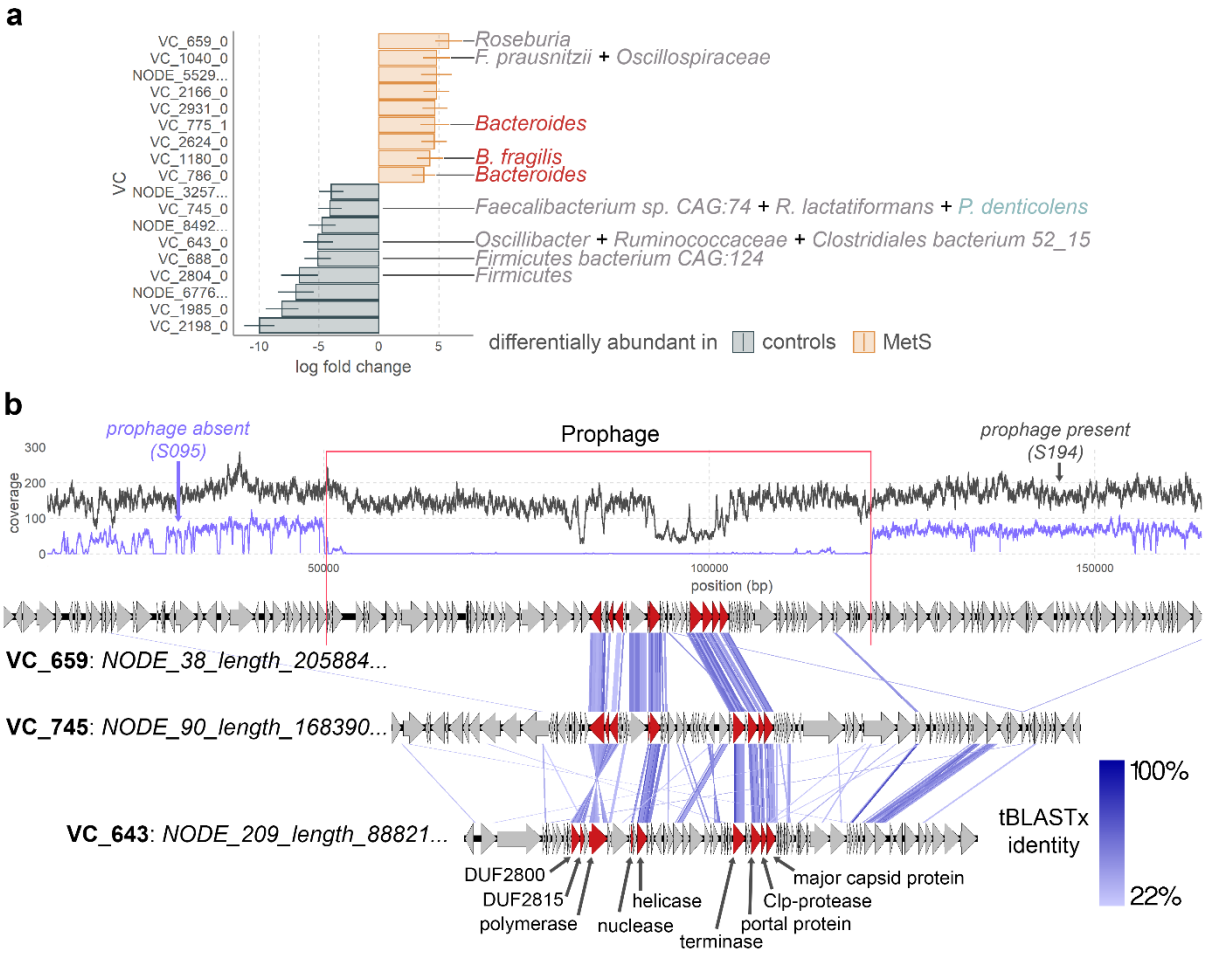

Figure 4: Among significantly differentially abundant VCs some are related. a ANCOM-BC analysis identified eighteen significantly abundant VCs with q ≤ 0.05. Error bars denote ANCOM-BC-supplied standard error. Host predictions are denoted where relevant and colored as follows: *Firmicutes;* grey, *Bacteroidetes;* red, *Actinobacteria*; green. For brevity only the lowest taxonomic level of the predictions is noted. For the full taxonomies, see Supplementary Table 2 and 4. The names of the four singletons is abbreviated. The full names are: NODE_3257_length_15024_cov_7.657693, NODE_5529_length_6063_cov_12.201232, NODE_6776_length_5490_cov_118.684269, and NODE_8492_length_5940_cov_10.538997. **b** Whole genome analysis of three contigs that belong to VC_659_0, VC_745_0 and VC_643_0. The VC_659_0 contig is zoomed in on the prophage region, for the entire contig, see Figure 6. The read coverage depth of this contig in two samples is displayed at the top, on in which the prophage is present (S194) and one in which it is absent (S095). The nine genes shared by all *Candidatus Heliusviridae* are colored red, and annotated at the bottom.

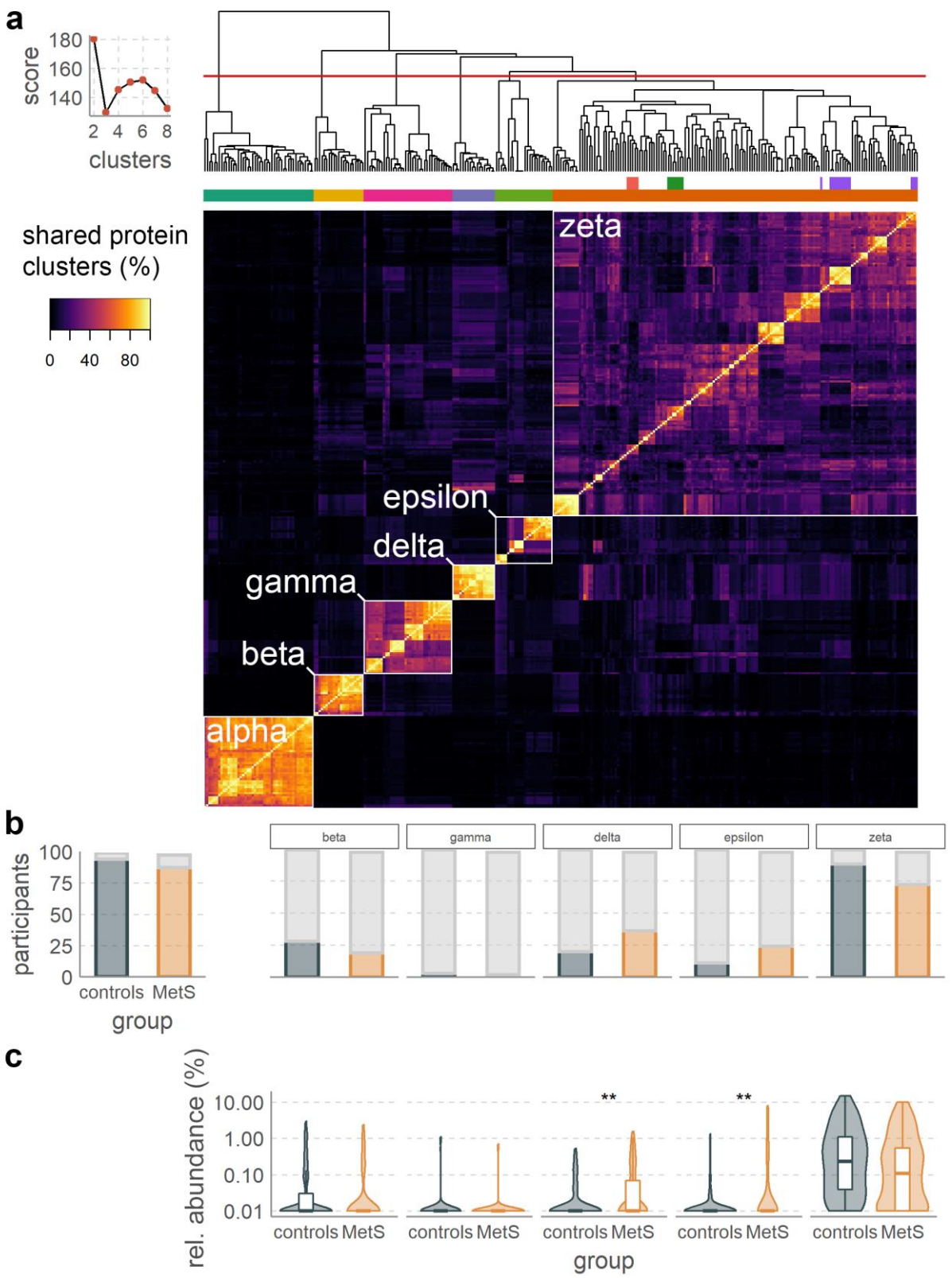

Figure 5: Three VCs that are hallmarks for either MetS or healthy control viromes are part of the widespread *Candidatus Heliusviridae* family of gut phages. a heatmap and hierarchical clustering of pairwise shared protein cluster values for 249 contigs from the current study and 51 previously isolated phages. The line graph shows the optimal number of clusters

as determined using the NbClust R package[100], and the dendrogram is cut to form six clusters. These six clusters are labeled as alpha, beta, gamma, delta, epsilon, and zeta subfamilies. The top row of colors beneath the dendrogram denote the differentially abundant VCs, from left to right: VC_745_0 (red), VC_659_0 (green), and VC_643_0 (purple). The bottom colors are according to the candidate subfamilies. **b** the prevalence of the *Candidatus Heliusviridae* (left) and the separate candidate subfamilies (right). **c** the relative abundances of the candidate subfamilies (the whole family was not significantly more abundant in either group and is thus not depicted). q-values are denoted as follows * ≤ 0.05, ** ≤ 0.01, *** ≤ 0.001, **** ≤ 0.0001.

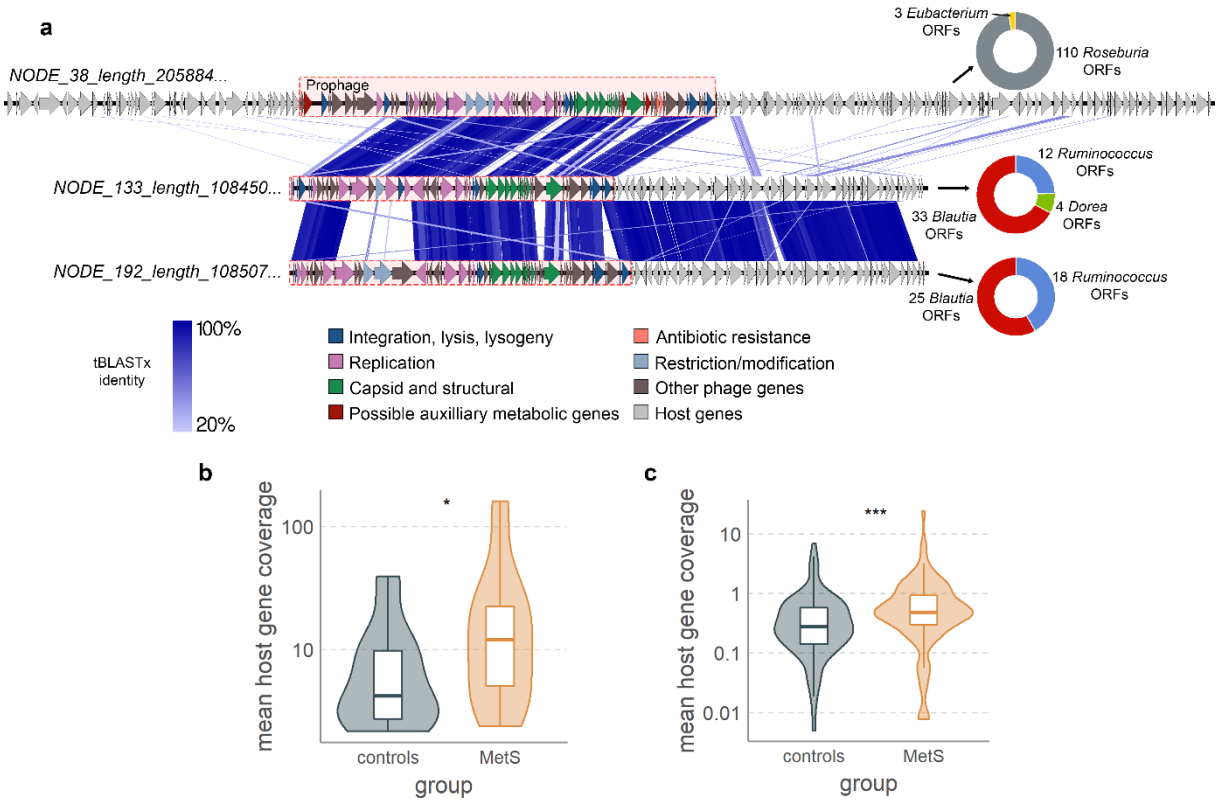

Figure 6: VC_659_0 infects *Roseburia* and *Blautia*, and carries possible auxiliary metabolic genes. a Whole genome alignment of three prophages contained within VC_659_0, with pie charts denoting the top BLASTp hit of all host genes on the contigs. **b** and **c** the mean coverage of host-derived regions in NODE_38 (**b**) and NODE_192 (**c**). Significance according to Wilcoxon signed rank test, p-values are denoted as follows * ≤ 0.05, ** ≤ 0.01, *** ≤ 0.001, **** ≤ 0.0001.

<u>Supplementary Figures</u>

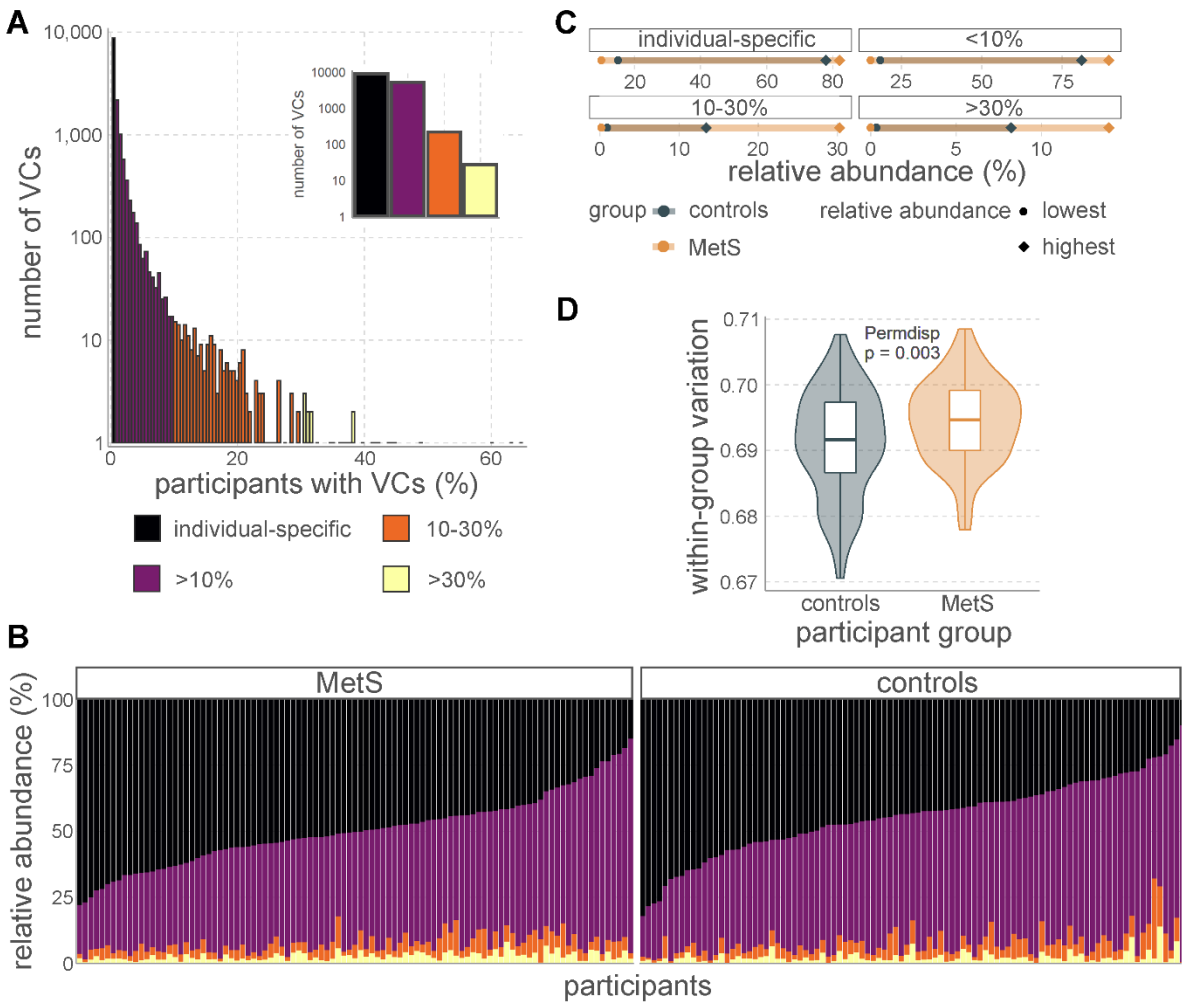

Supplementary Figure 1: Overview of the viromes show more variability among MetS participants. a Histogram of VCs by number of participants that they are found in shows most VCs are individual-specific. The inset is the same dataset with one bar for each category shown in the legend. **b** Stacked bar charts of community composition show high inter-individual virome diversity. Color legend is identical to (A). **c** Comparisons show that participants with the highest and lowest relative abundance in each VC category all belong to the MetS group. **d** MetS participants have significantly higher within-group variation, as measured by permdisp on Bray-Curtis dissimilarities.

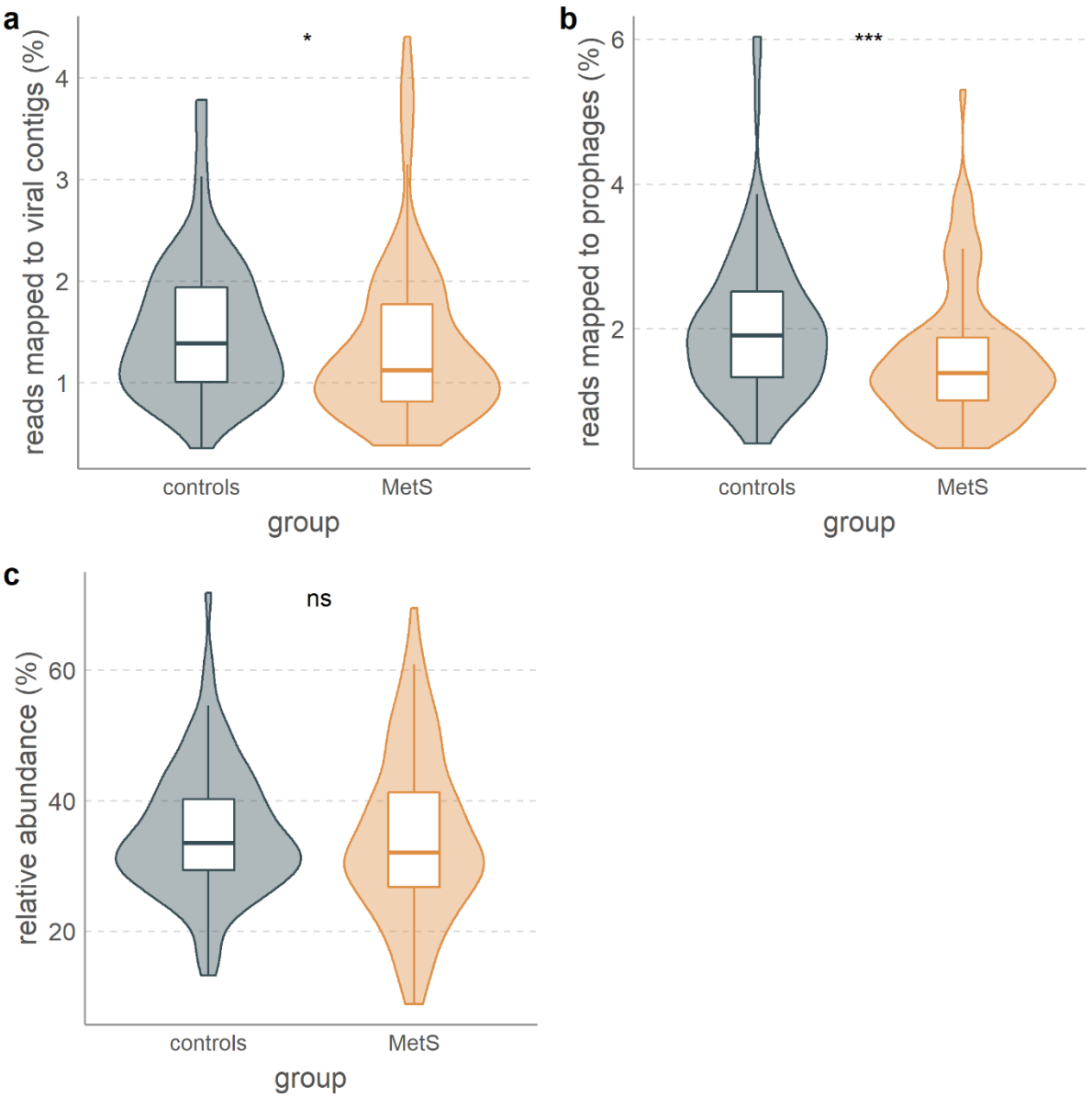

Supplementary Figure 2: Differences in total phage abundance and potential temperate phage abundance. a total phage abundance, as shown by the percentage of reads that map to viral sequences. **b** significantly more reads map to bacterial contigs that contain prophage-like sequences. **c** no significant difference in relative abundance of VCs that carry integrase genes. Stars denote significance according to the Wilcoxon signed rank test. * ≤ 0.05, ** ≤ 0.01, *** ≤ 0.001, **** ≤ 0.0001.

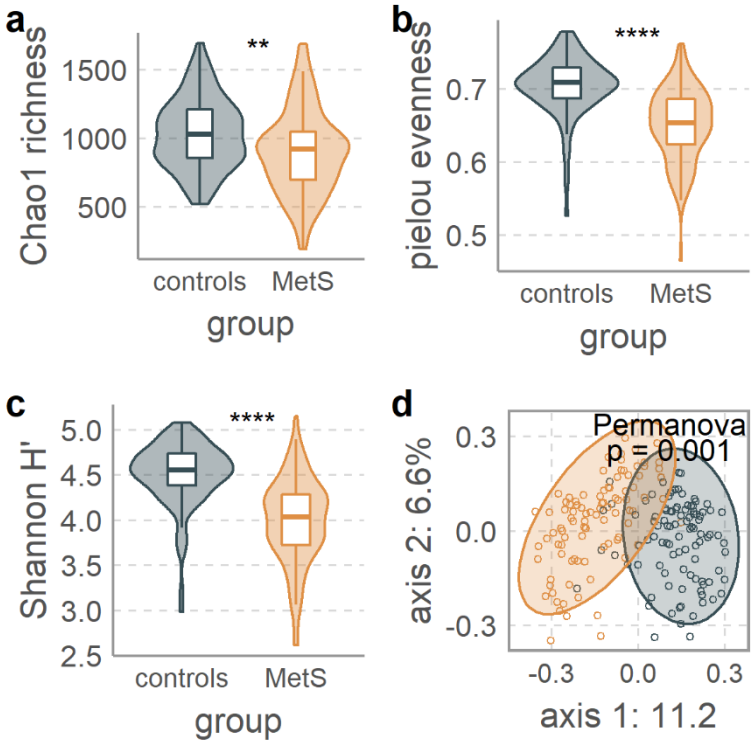

Supplementary Figure 3: Gut bacterium populations are altered in MetS. a MetS-associated decreased bacterial species richness is evidenced by the Chao1 index. **b** decreased bacterial pielou evenness measurements. **c** significantly decreased bacterial α-diversity measured by Shannon diversity. **d** clear separation between bacterial populations of MetS and control participant as shown by β-diversity depicted in a principal coordinates analysis (PCoA) of Bray-Curtis dissimilarities. Statistical significance in A-C is according to the Wilcoxon signed rank test, where p-values are denoted as follows: ns not significant, * ≤ 0.05, ** ≤ 0.01, *** ≤ 0.001, **** ≤ 0.0001.

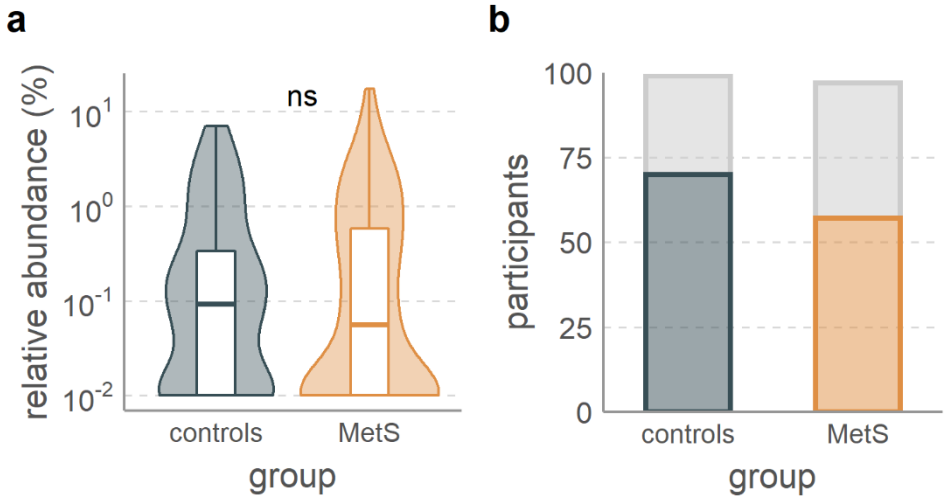

Supplementary Figure 4: Non-significant differences in crAss-like phage populations. a relative abundance of crAss-like phages in controls and MetS. **b** the number of participants in which crAss-like phages were present.

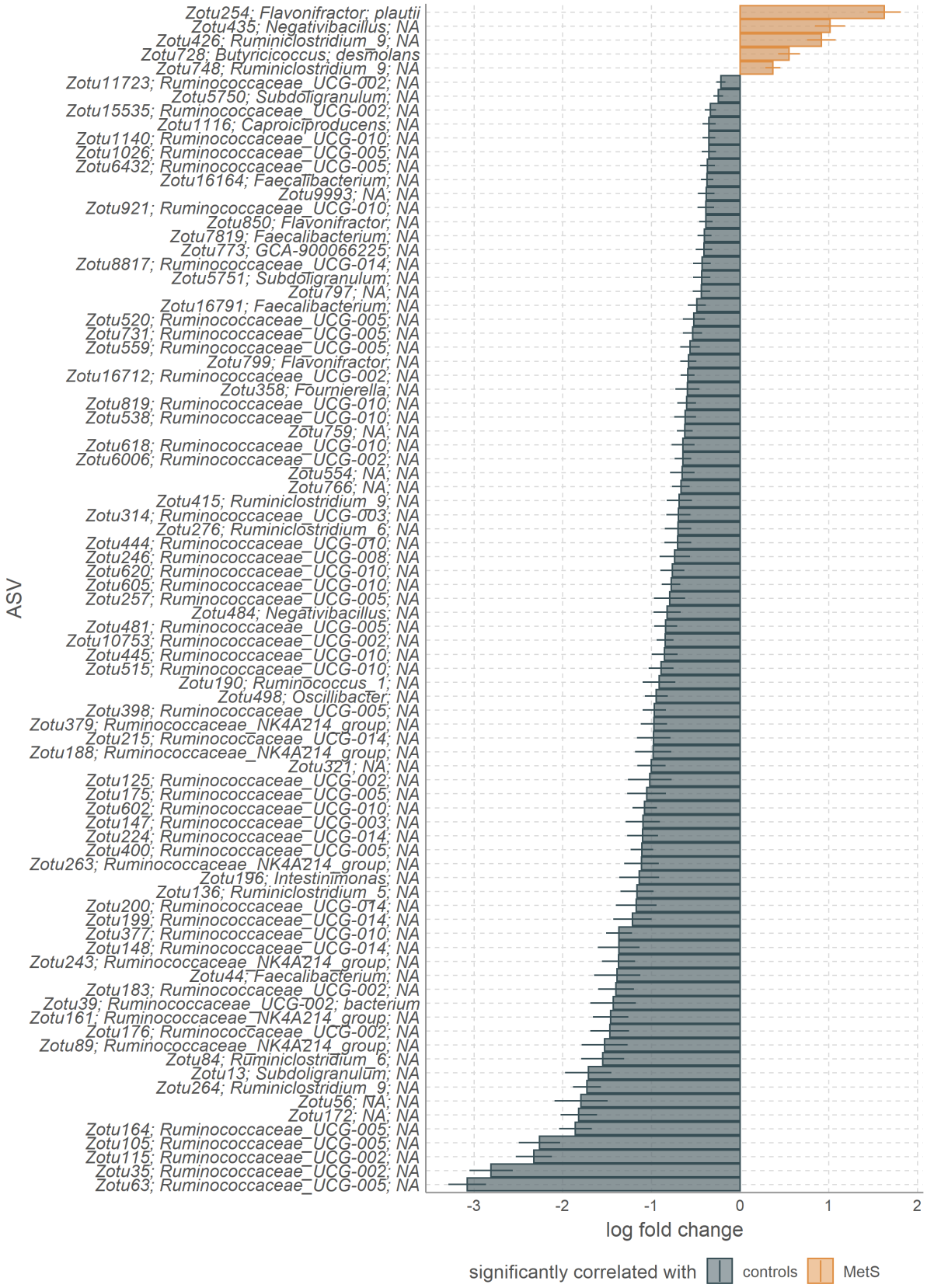

Supplementary Figure 4: ANCOM-BC analysis results of significantly differentially abundant *Ruminococcaceae* ASVs.

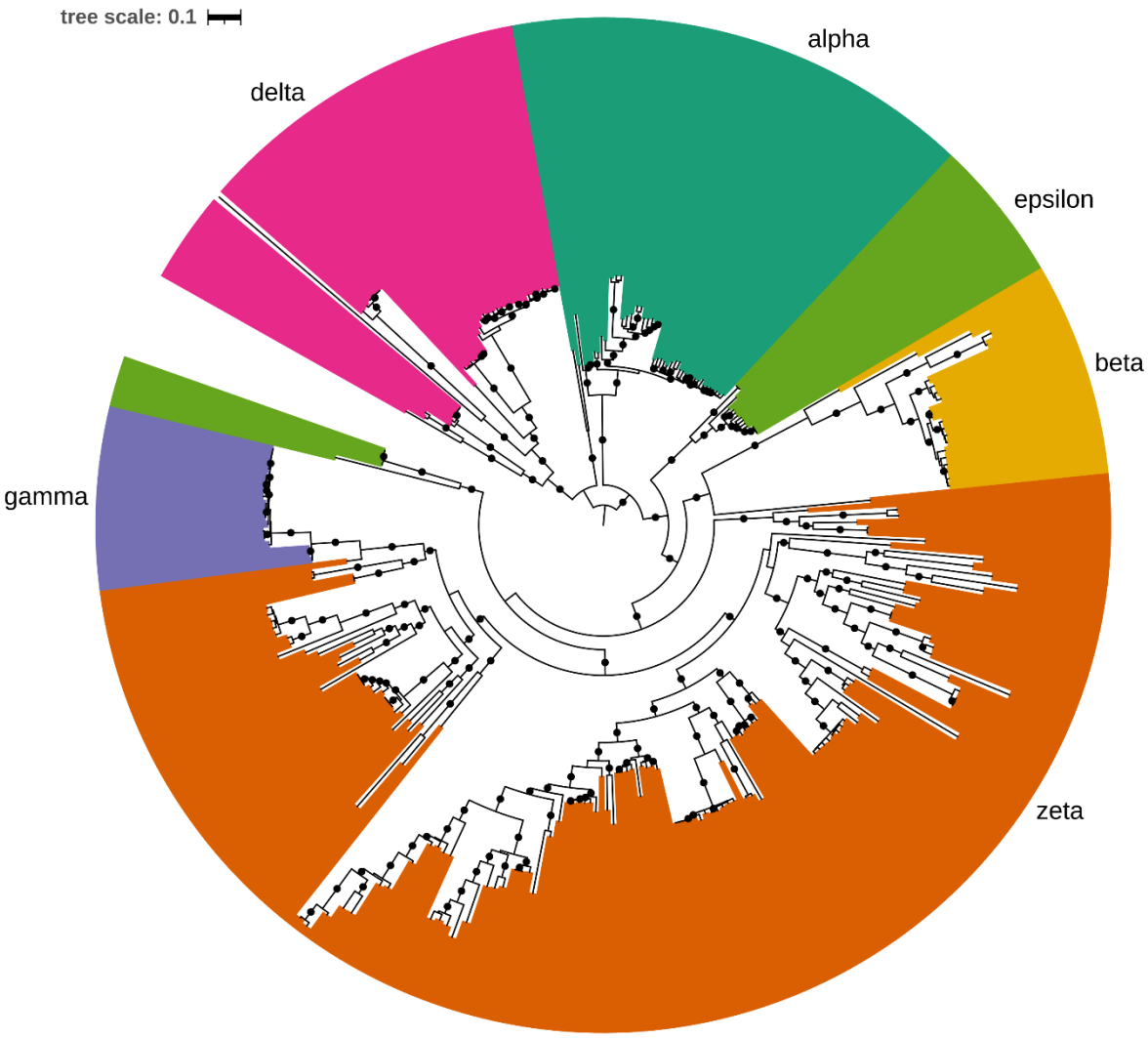

Supplementary Figure 6: A midpoint-rooted approximate maximum likelihood tree made from the concatenated alignments of the nine universally shared *Candidatus Heliusviridae* genes, with colors denoting the groups. Dots represent bootstrap values of ≥95.